INTERNATIONAL ATOMIC ENERGY AGENCY
UNITED NATIONS EDUCATIONAL, SCIENTIFIC AND CULTURAL ORGANIZATION

INTERNATIONAL CENTRE FOR THEORETICAL PHYSICS
34100 TRIESTE (ITALY) - P.O.B. 586 - MIRAMARE - STRADA COSTIERA 11 - TELEPHONE: 2240-1
CABLE: CENTRATOM - TELEX 460392-1

SMR.300/ 59

College on Medical Physics
(10 October - 4 November 1988)

Special Dosimetric Problems in Mammography

W. PANZER

GSF, Munich, GFR

** These notes are intended for internal distribution only

Special Dosimetric Problems in Mammography

W. Panzer

Institut für Strahlenschutz

Gesellschaft für Strahlen- und Umweltforschung
München - Neuherberg

Since mammography was proposed as a screening method for the early detection of breast cancer in the late sixties /8/ it became object to countless investigations dealing with the dosimetric aspects of this examination /1, 3, 7, 9, 11, 14, 16, 23, 26/. However, dosimetric aspects appeared in a different problematic context and in different ranking among other physical or medical considerations thus giving a rise to a confusing variety of

- terms or concepts in which dose is expressed
- methods how to evaluate dose
- published dose values.

There are mainly three fields in which dosimetric considerations and measurements play an essential part:

1) Optimisation of mammographic procedures
2) Quality control
3) Assessment of risk related dose to patients

Optimisation of technical and physical parameters in mammography

Aim of these attempts which generally occur on laboratory or research level is either to increase the detectability of the most important diagnostic details (microcalcifications, small masses, engorged ducts and thickened skin) at reasonable or acceptable dose levels or to reduce the dose to patient without deterioration of image quality or to achieve both improvements to a certain degree. The most crucial parameters in this context are:

- anode material
- filtration
- tube voltage
- properties of the image detectors
  - sensitivity
  - sharpness
  - contrast
  - noise
- geometric conditions
- cassette materials
- anti-scatter grids.

The list of these parameters is rather the same like with other X-ray examinations. But each of these parameters gains a higher importance because of the low radiation energies used in mammography, the comparatively high doses to patients and the high demand for detectability of very small details and details of rather poor contrast.

Quality control

In the course of quality control programs /1/ and field studies /7, 15, 20, 26/ on a large scale

- radiation output and reproducibility
- radiation quality
- performance of automatic exposure units

were examined by dosimetric methods and image parameters like

- average optical density
- contrast
- resolution
- detectability of test details

were correlated to dose values. To find out about them and to put an end to the most frequent technical failures for unnecessary high exposures and poor images in daily mammography all these measurements or tests must be performed under routine conditions and at as many facilities as possible. This, however, needs to make a compromise between dosimetric precision and easy handling and low-cost of the dosimetric devices used.

Assessment of risk related dose to patients

Because mammography is proposed not only for symptomatic patients, but also as a screening method, there is a strong need for recommendations concerning the frequency, the age at which screening should start and the selection of those women who should undergo screening mammography. The knowledge of risk related dose values which are typical for the various

mammographic techniques is therefore essential as a basis for risk - benefit estimations. Such dose values drop into advices on the radiographic techniques and in the proposals for dose limits which should not be exceeded. So, for example, the Health Council of the Federal Republic of Germany limits the breast dose for one mammogram to 5 mGy.

Dosimetric instrumentation

Ionisation dosemeters

The most suitable systems for precise dose measurements free in air or in phantoms are plane-parallel soft X-ray chambers with thin entrance windows and small collecting volumes (fig. 1). They are sensitive enough to produce measurable signals during a single exposure and, on the other side do not suffer from saturation losses. Because of their small dimensions in direction of the beam they allow for correct measurements of surface doses and depth doses. The energy dependence in the energy range considered is negligible, thus exact knowledge of radiation quality, for the purpose of dose measurement, is not necessary. In addition with X-rays from molybdenum anodes filtered by molybdenum the radiation quality is highly determined by the characteristic K-radiation of molybdenum and the voltage-dependent contribution from the Bremsstrahlung is by far less than with other diagnostic radiation qualities (fig. 2). The situation is different when tungsten anodes are used or molybdenum anodes together with aluminum filters (fig. 3), but the energy independence of the ionisation chamber will not be affected by this.

However, a geometric effect with these chambers must be considered: The collecting volume is embedded in a bulky chamber body. When such a chamber was calibrated free in air against a free air chamber (like it happened or still happens in Primary Standard Laboratories) a certain amount of radiation scattered by the chamber body into the collecting volume contributed to the dosemeter reading and was included into the calibration factor. Now, when the chamber is used within a phantom the contribution from the phantom material substituted by the chamber body will be missing and so the measurement will undervalue the real dose within the phantom. An effect which has to be corrected for, at least in precise measurements because it can reach 6% and more (tab. 1).

Table 1: Correction factors k_{ap} when free air calibrated chambers are used within phantoms /5/

Tube voltage KV	Total filtration Be mm	Total filtration Al mm	Half value layer mmAl	k_{ap} M 23344 (PTW) NE 2536	k_{ap} M 23342 (PTW) NE 2532
15	1.5	+ 0.05	0.07	1.00	1.00
20	1.5	+ 0.15	0.11	1.01	1.01
30	1.5	+ 0.50	0.36	1.04	1.03
40	1.5	+ 0.80	0.71	1.065	1.05
50	1.5	+ 1.0	0.94	1.075	1.06
70		4.0	2.8	1.10	1.075
100		4.5	4.4	1.105	1.08

The determination of absorbed dose in a phantom follows then the relation:

$$D_p = M \cdot f_c \cdot k_{ap} \cdot t_{pa} \qquad (1)$$

D_p : Absorbed dose in phantom material
M : Instrument-reading (corr. f. air density)
f_c : Calibration factor (air kerma / reading)
k_{ap}: Correction factor (tab. 1)
t_{pa}: $(\mu_{en}/\rho)_{phantom} / (\mu_{en}/\rho)_{air}$ (tab. 2)

Table 2: Values t_{pa} to convert air kerma into absorbed dose in phantom /5/

Tube voltage KV	Total filtration Be mm	Total filtration Al mm	Half value layer mmAl	t_{pa} (water)
10	1.5		0.03	1.054
15	1.5	+ 0.05	0.07	1.048
20	1.5	+ 0.15	0.11	1.041
30	1.5	+ 0.50	0.36	1.028
40	1.5	+ 1.80	0.71	1.022
50	1.5	+ 1.0	0.94	1.019
70		4.0	2.8	1.019
100		4.5	4.4	1.029

When a chamber is used which was calibrated within a phantom and in terms of absorbed dose to water, relation (1) changes into:

$$D_p = M \cdot f_c \cdot t_{pw} \cdot B_p/B_w \qquad (2)$$

D_p : Absorbed dose in phantom material
M : Instrument-reading (corr. f. air density)
f_c : Calibration factor (absorbed dose to water / reading)
t_{pw}: $(\mu_{en}/\rho)_{phantom} / (\mu_{en}/\rho)_{water}$ (tab. 3)

B_p/B_w: Backscatter ratio between phantom material and water. The values are very close to unity.

Table 3: Values for t_{pw} to convert absorbed dose in water into absorbed dose in tissue /5/

Tube voltage KV	Total filtration Be mm	Total filtration Al mm	Half value layer mmAl	t_{pw} skin	t_{pw} muscle	t_{pw} fat
10	1.5		0.03	0.885	0.995	0.565
15	1.5	+ 0.05	0.07	0.888	1.005	0.563
20	1.5	+ 0.15	0.11	0.890	1.01	0.561
30	1.5	+ 0.50	0.36	0.896	1.025	0.560
40	1.5	+ 0.80	0.71	0.899	1.03	0.562
50	1.5	+ 1.0	0.94	0.900	1.035	0.565
70		4.0	2.8	0.912	1.04	0.595
100		4.5	4.4	0.922	1.04	0.635

If in case a chamber with an older calibration in terms of exposure is available, absorbed dose to phantom material follows the relation:

$$D_p = M \cdot f_c \cdot k_{ap} \cdot W/_e \cdot t_{pa} \qquad (3)$$

D_p : Absorbed dose in phantom material
M : Instrument reading
f_c : Calibration factor (exposure / reading)
$W/_e$: 8.69 mGy/R
t_{pa}: $(\mu_{en}/\rho)_{phantom} / (\mu_{en}/\rho)_{air}$ (tab. 2)

There are only few situations in dosimetry in mammography where the demand for accuracy compels the strict application of correction factors, most of them close to unity. These are for example the measurement of surface and depth dose in materials intended for use as breast phantom or data assessment for dose calculations. But it should be practised for the sake of a

better understanding of the dosimetric procedures and to avoid unnecessary errors during the first steps of dosimetric activities, as the calibration of TL-dosemeters for field studies.

Solid state dosemeters

Thin layers of CaF, LIF, $CaSo_4$ or LIB_4O_7 can also be used with some limitations for dose measurements in mammography /14, 16, 22, 26/. The increasing energy dependence toward very low energies (fig. 4) is caused by the poor tissue- or air equivalence of the dosemeter material. Problems might arise from that, when output or surface dose measurements are performed with radiation from tungsten anodes and the values of tube voltage and filtration are not sufficiently known (half value layer range 0.3 - 1 mmAl). In the depth of the phantom or on the exit surface the radiation quality (half value layer range some mmAl) tends to lie in the flat part of the response curve. With radiation from molybdenum anodes filtered by molybdenum the problem does not arise, because of the dominating contribution from the characteristic K-radiation from molybdenum the radiation quality is restricted to a very narrow range (half value layer range 0.3 - 0.4 mmAl) independently from tube voltage. Errors also can result from a pronounced directional dependence. So the dosemeter should always be calibrated under conditions as close as possible to those where the dosemeters are used. Large variations of sensitivity even within the same charge of probes demand for an individual calibration of each dosemeter. Poor reproducibility, fading,

Inconstancies of the reading equipment which cannot always be avoided lead to generally higher cross errors with TL-dosemeter measurements. But thus drawback is compensated by their high utility in field studies, quality control programs and on-patient measurements.

Phantoms

The most crucial dosimetric problem in mammography is the selection of a suitable phantom material and the design of a phantom which is similar to an average breast with regard to thickness, density and elementary composition. In the range of the very low photon energies used in mammography there is a strong dependence of absorption and scattering from the density and atomic number of the material irradiated. Large differences in dose will be observed when different phantom materials are used. The situation is still more complicated by the fact that in a collective of patients there is not only a wide range of object thickness (thickness of the compressed breast), but also a large variation in composition of the breast out of parenchymal tissue, connective tissue and fatty tissue. So for the same object thickness changes in entrance dose by a factor of 3 - 4 can be observed. This is shown in fig. 5 where entrance doses from a collective of 213 patients are plotted against object thickness and fitted by an exponential curve /19/. Such distributions depend on the age of the patients forming the collective and other authors might find out different distributions. Figs. 6 - 8 demonstrate how

other materials proposed for dosimetric breast phantoms agree with a real patient collective /19/. There is no ideal material available which allows for the simulation of breast tissue by a homogeneous phantom over the whole range of object thickness. This renders the development of a standard breast phantom so diffcult and makes understandable why there exists such a confusing variety of proposals for breast phantoms. However, as it follows from fig. 7 the curve for a rather simple material like Perspex (Lucite) cuts the fitting curve of the patient collective at medium object thickness. Since Perspex is easily available, has good reproducibility in its composition and causes no problems in handling and machining it can be proposed as a standard phantom for a medium sized breast for Quality Control and optimisation of mammographic techniques.

Determination of dose to patient

Entrance dose as it was employed in the figures above is a rather poor descriptor of dose to patient. But it is easily measurable and widely used in context with Quality Control, field studies and optimisation of mammographic techniques. By measuring entrance dose one can demonstrate trends, detect failures or describe the impact of technical improvements. However, in terms of entrance dose the consequences for dose to patient might be severely over- or underestimated and finally it cannot be considered as a risk related dose at all. Dose to patient is best characterised by average breast dose D_m or by average glandular dose D_g /12, 13, 23/. While D_m includes

also the scarcely radiation sensitive skin and adipose tissue, D_g considers only the glandular tissue which is more vulnerable to radiation cancerogenesis. The use of average organ doses values as it is also practised in other radiation protection fields, is in consistency with the assumption of a linear dose - effect relation. The determination of D_m or D_g is facilitated by the following facts:

- The object is rather homogeneous and can simply be modeled by a plane-parallel phantom (fig. 9).

- Fieldsizes are small and their influence on organ dose is negligible because of the low photon energies.

- Focus to skin distance is large compared with object thickness. Size and shape of the irradiated volume does not depend on it (with the exception of magnification techniques).

- Depth dose curves follow closely exponential curves (fig. 10) /11, 17, 18, 19, 22/. This holds true especially for radiation from molybdenum anodes, but also for radiation from tungsten anodes.

So D_m or D_g can be calculated straight forward from measured values of the entrance dose D_E and the exit dose D_A:

$$D_m = \int_0^a D_E \cdot \exp(-\mu x)dx/a$$

a: thickness of phantom or breast
μ: $\ln(D_E/D_A)/a$

$$D_m = D_E[1-\exp(-\mu a)] / (a \cdot \mu) \qquad (4)$$

or:

$$D_g = \int_f^{a-f} D_E \exp(-\mu x)dx / (a - 2f)$$

a: thickness of phantom or breast
μ: $\ln(D_E/D_a)/a$
f: thickness of skin and adipose tissue

$$D_g = D_E [\exp(-\mu f)-\exp(-\mu(a-f)] / (\mu(a-2f)) \qquad (5)$$

The error introduced by assuming the values for f can be estimated from fig. 11 where D_g for a phantom of 5 cm thickness is calculated for varying values of f.

The values for D_m and D_g as calculated from equation 4 and 5 appear in a first step in the same unit in which the dosemeter for the measurement of D_E and D_A was calibrated (exposure, air Kerma or absorbed dose in water). They must then be converted into absorbed dose in the tissue of interest. Numerous authors proposed very different conversion factors, depending on which content of fatty tissue in the breast they took into account /10, 11, 17/. However, this considerations are misleading because the parenchymal tissue is the tissue at risk and not the fat cells. Because of the low photon energies the range of secondary electrons responsible for the energy transfer is so short (< 10 µm) that an energy transfer from fat cells into parenchymal cell (and vice versa) is unprobable. So for the energy depositions in the parenchyma

only the absorption in parenchyma is responsible and the mass-energy-absorption-coefficients of parenchyma must be used. These are very close to those of water and thus the D_m and D_g can be expressed in absorbed dose in water /21/.

This method to determine risk related organ doses in mammography, either applied to phantoms or to patients seems to be rather simple compared with other methods reported including Monte Carlo calculations and the use of very sophisticated phantom materials /3, 4, 6, 24, 25/. However, the results are not less reliable. Because the main hindrance for an exact dosimetry, the restricted possibilities to develop a standard phantom, exists also with the other methods.

A field study for the evaluation of dose values in mammography

Dose reduction methods like the use of high sensitivity film-screen combinations instead of non-screen film have become more and more common also in Germany. To find out the effect of this trend on the dose required for an examination a survey was conducted. About threehundred hospitals and small clinics in Bavaria were approached for cooperation and finally about 170 agreed to participate.

Test procedure

A simple test phantom was sent to the participants by mail. It consisted out of a plastic box 4 cm high and 10 cm

diameter, large enough to completely cover the chamber area of the automatic exposure control units. After filling it with water up to an indicated height of 3.5 cm this water layer for the purpose of this test represents a medium sized breast as can be seen from fig. 7 with all the restrictions mentioned above. They had to expose it together with the film or film-screen combinations commonly used at the unit. In addition the participants were asked to answer a short questionnaire to specify the conditions of film exposure and processing, types of films and screen and anti-scatter grids used.

The developed films and two sets of three $CaSO_4$ TL-dosemeters mounted on the entrance- and exit surface of the phantom were returned for evaluation of film density and surface dose. $CaSO_4$ proved to be sufficiently energy-independent in the energy range of interest between 15 and 50 keV. The TL-dosemeters were individually calibrated under test conditions by means of a soft X-ray ionisation chamber.

Results

From the participants in the survey:

- 53% used films without screens
- 36% used film-screen combinations with grid
- 11% used film-screen combinations without grid.

Xeromammography was applied by just one facility. 98% of the facilities were equipped with automatic exposure control units and 92% with automatic film processing.

The distributions of the measured entrance and exit doses are shown in fig. 12. The wide spread of values for both entrance- and exit-dose and the wide overlapping of distributions for image recording systems of very different speed is not unexpected for routine mammographic examinations. Its extent, however, is surprising in this field study, because the participants exposed the same standardised phantoms and used very similar radiation qualities. In the case of a Mo-anode and a Mo-filter a change of tube voltage scarcely affects the spectrum of the incoming radiation and only slightly the spectrum of the transmitted radiation through a medium sized phantom. This indicates that, besides the differences in speed of the various makes, the main effect on dose values results from the optical density of the films preferred by the participants as a result of their personal practice and experience, and the conditions of film processing.

Average glandular doses were calculated from the entrance and exit doses, assuming a 0.5 skin and apidose tissue layer. The results for the various image receptor systems are listed in table 4.

Table 4: Average glandular doses [mGy]

	1.Quartile	Median	3.Quartile
Film	10.5	16	22
Film screen with grid	4.2	6.6	10.1
Film screen without grid	1.8	3.82	4.9

References

1.) Jans, R.G. et al. (Bent Study, Results), Radiol., 132, 197-200 (1979)

2.) Birch, R., Marshall, M., Ardran G.M., Catalogue of spectral dates for diagnostic x-rays. HPA, Scientific Report Series 30, London (1979)

3.) Boag, J.W., Stacey, A.J., Davis, R., Brit. J. Radiol. 49, 253-261 (1976)

4.) Dance, D.R., Phys. Med. Biol. 25, 25-37 (1980)

5.) DIN 6809, Teil 4: Klinische Dosimetrie; Anwendung von Röntgenstrahlen mit Röhrenspannungen von 10 bis 100 KV in der Strahlentherapie und in der Weichteildiagnostik. (1984)

6.) Doi, K., Chan, H.P., Radiol. 135, 199-208 (1980)

7.) Fitzgerald, M., White, D.R., White, E., Young, J., Brit. J. Radiol. 54, 212-220 (1981)

8.) Gershon-Cohen, J., Radiol. 88, 663-670 (1967)

9.) Giera, W., Paterok, E.M., Prestele, H., Säbel, M., Weishaar, J., Röntgenpraxis 35, 445-453 (1982)

10.) Hammerstein, G.R. et al., Radiol. 130, 485-491 (1979)

11.) Karlson, M., Nygren, K., Wickmann, G., Hettinger, G., acta radiol., Ther. Phys. Biol. 15, 252-258 (1976)

12.) NCRP-Report No 66: Mammography. NCRP, Washington D.C. (1980)

13.) NCRP-Report No 85: Mammography - A User's Guide. NCRP, Washington D.C. (1986)

14.) Panzer, W., Regulla, D.F., Scheurer, C., Brit. J. Radiol., Suppl. 18, 108-110 (1985)

15.) Panzer, W., Drexler, G., Widenmann, L., Platz, L.: Spektren und Dosiswerte in der Mammographie. GSF-Bericht S-518 (1978)

16.) Säbel, M., Ruff, A., Weishaar, J., Fortschr. Röntgenstr. 128, 616-622 (1978)

17.) Schneider, G., Kindl, P., Spreizer, H., Fortschr. Röntgenstr. 128, 82-86 (1978)

18.) Shrivastava, P.N., Radiology 140, 483-490 (1981)

19.) Säbel, M., Fortschr. Röntgenstr. 134, 250-254 (1981)

20.) Scheurer, C., Panzer, W., Regulla, D.F., Medizinische Physik 84 (Ed.: Th. Schmid), 607-610, Nürnberg (1984)

21.) Stanton, L., Villafana, T., Day, J.L., Lightfoot, D.A., Invest. Radiol. Vol 13, 4, 291-297 (1978)

22.) Stanton, L., Day, J.L., Brattelli, S.D., Lightfoot, D.A., Med. Phys. 8, 792-798 (1981)

23.) Stanton, L., Villafana, T., Day, J.L., Lightfoot, D.A., Radiology 150, 577-584 (1984)

24.) White, D.R., Phys. Med. Biol. 22, 889-899 (1977)

25.) White, D.R., Martin, R.J., Darlison, R., Brit. J. Radiol. 50, 814-821 (1977)

26.) Zuur, C., Zoetelief, J., Visser, A.G., Broerse, J.J., Brit. J. Radiol., Suppl. 18, 110-114 (1985)

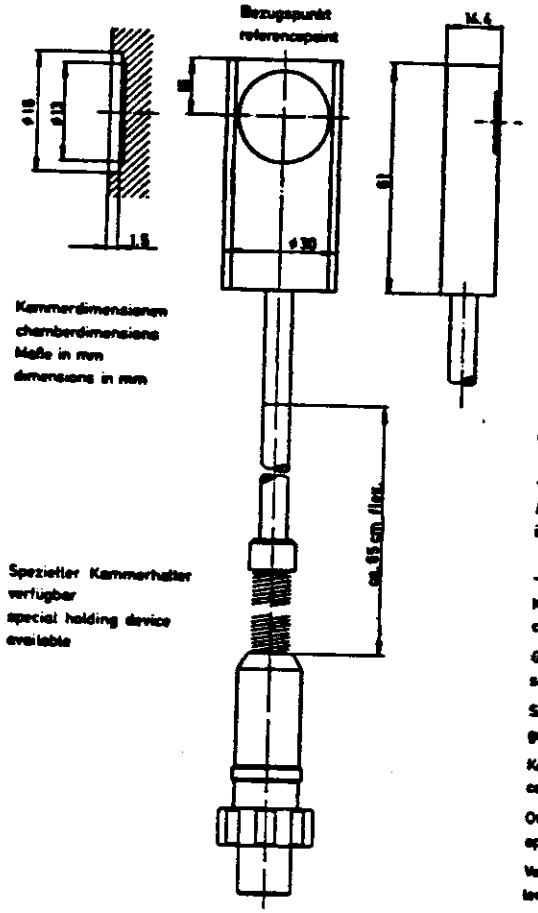

Volumen	volume	0.30 cm³
Strom	current	$7 \cdot 10^{-9}$ A Gy^{-1} s
Leckstrom	leakage	$\leq 1 \cdot 10^{-14}$ A
Kammerspannung	polarizing voltage	max. 300 V
Schutzpotential	guard potential	max. 100 mV
Kabelbestrahlung	cable leakage	10^{-12} A Gy^{-1} s cm^{-1}
Membranmaterial	membrane material	CH_2
Membrandicke	membrane thickness	0.03 mm
Flächengewicht	weight per unit area	2.5 mg cm^{-2}
Temperaturbereich	range of temperature	+10 – +40° C
Rel. Luftfeuchte	rel. air humidity	≤ 75 %

Max. Dosisleistung bei kont. Bestr. max. exposure rate at cont. irrad.	150 V 300 V	Sättigung 99 % saturation	20 Gys^{-1} 80 Gys^{-1}	98.5 %	10 Gys^{-1} 40 Gys^{-1}
Max. Dosis pro Bestrahlungspuls max. exposure per irradiation pulse	150 V 300 V	Sättigung 99 % saturation	1.2 mGy 2.4 mGy	98.5 %	0.5 mGy 1.2 mGy
Ionenflugzeit ion collectiontime	150 V 300 V				0.12 ms 0.08 ms

Konstruktion: Schutzring bis zum Meßvolumen
construction: guardring up to measuring volume

Geeignet für Gebrauch in Festkörperphantomen
suitable for use in solid phantoms

Schutzring und alle leitenden, äußeren Teile an Massepotential
guardring and all conductive outerparts at masspotential

Kammerspannung nur über ~1MΩ Schutzwiderstand anlegen
connect polarizing potential only with current limiting resistor of ~1MΩ

Offenes Meßvolumen, ohne Kontrollvorrichtung ist Luftdichtekorrektur nötig
open chambervolume, without checkdevice air density correction is neccessary

Verlängerungskabel bis 100m verfügbar
lengthening cable up to 100m available

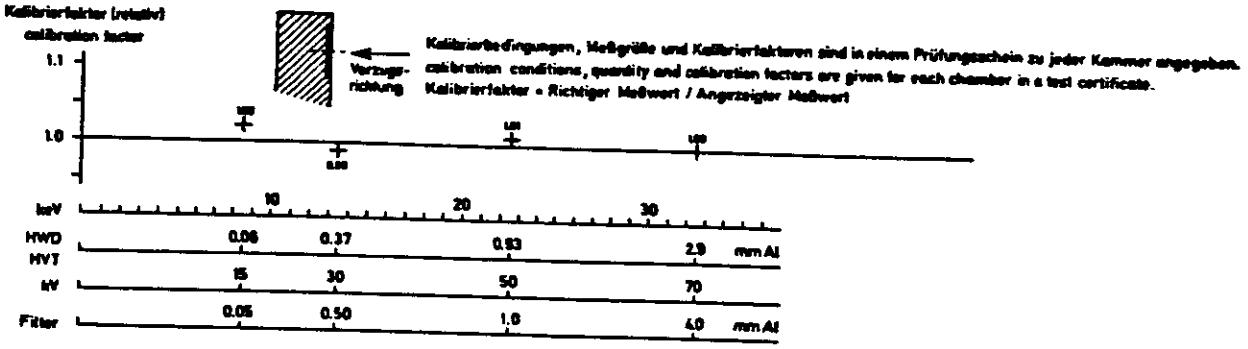

Fig. 1: Specifications of soft X-ray chamber for use in mammography

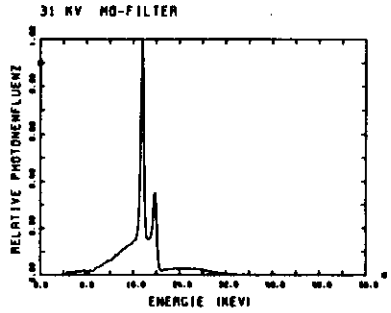

31 KV, 0.03 mm Mo-filter

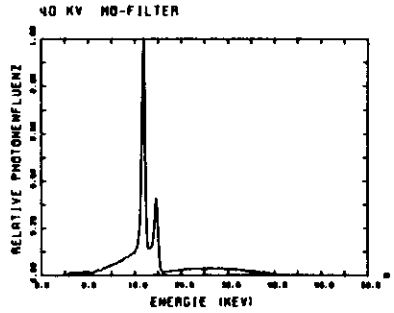

40 KV, 0.03 mm Mo-filter

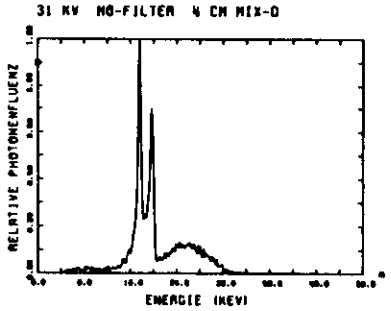

31 KV, 0.03 mm Mo-filter
4 cm phantom (MIX D)

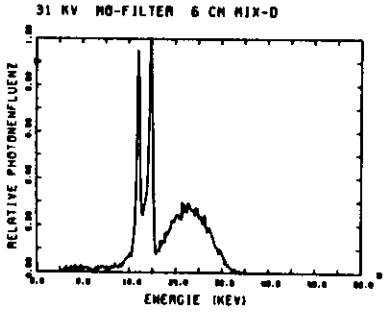

31 KV, 0.03 mm Mo-filter
6 cm phantom (MIX D)

Fig. 2: Spectral distributions in mammography. Relative photon fluence vs. photon energy (keV)

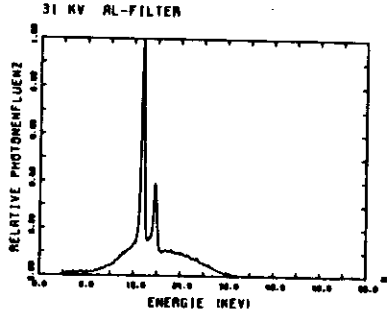

31 KV, 0.5 mm Al-filter

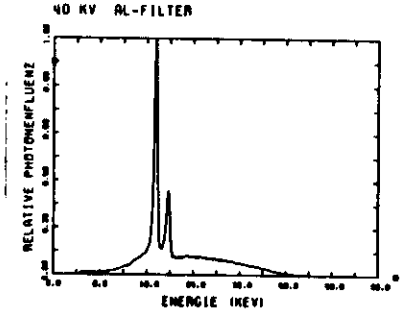

40 KV, 0.5 mm Al-filter

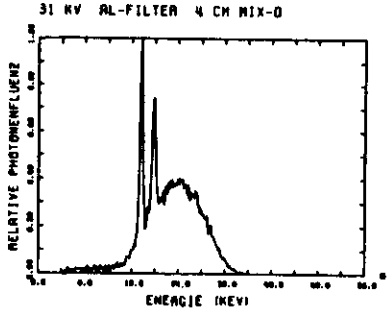

31 KV, 0.5 mm Al-filter
4 cm phantom (MIX D)

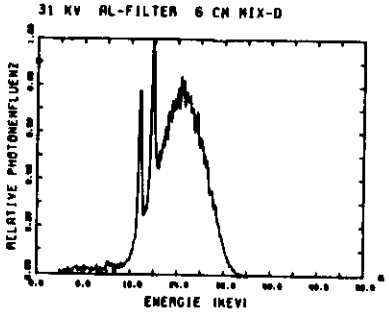

31 KV, 0.5 mm Al-filter
6 cm phantom (MIX D)

Fig. 3: Spectral distributions in mammography. Relative photon fluence vs. photon energy (keV)

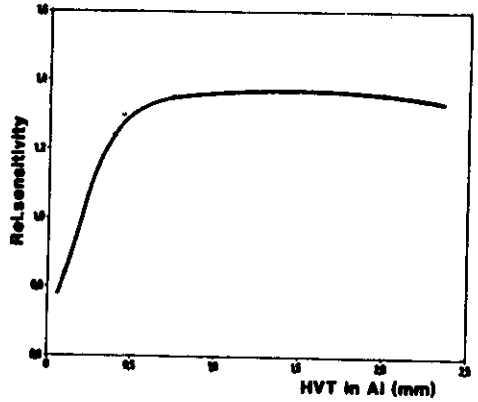

Fig. 4: Energy dependence of TL-material (LiF)

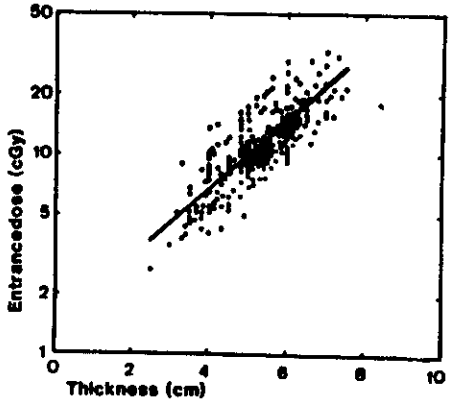

Fig. 5: Entrance dose vs. object thickness /19/. (30 KV, Mo-anode, 0.03 mm Mo-filtration, entrance dose: 122* ± 58 mGy, exit dose: 3.5 mGy, Kodak Definix Medical, Object thickness: 5.2* ± 1.0 mm; *mean value ± standard deviation)

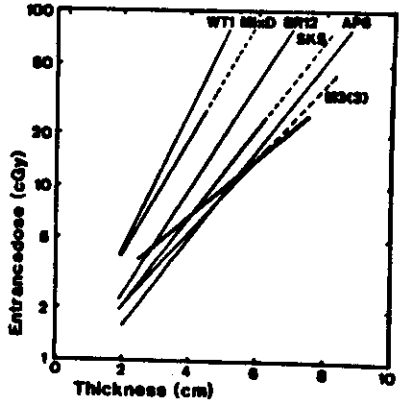

Fig. 6: Tissue equivalence of various phantom materials /19/

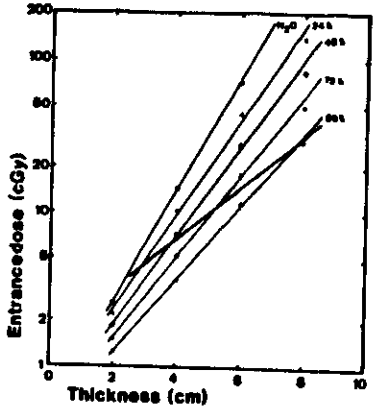

Fig. 7: Tissue equivalence of water-alcohol mixtures /19/

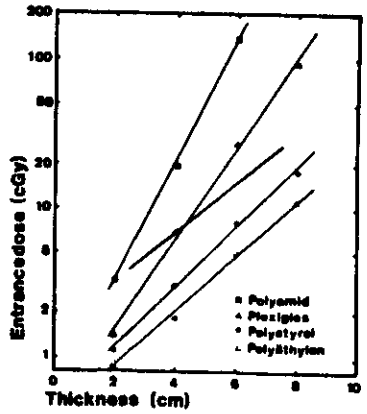

Fig. 8: Tissue equivalence of various plastics /19/

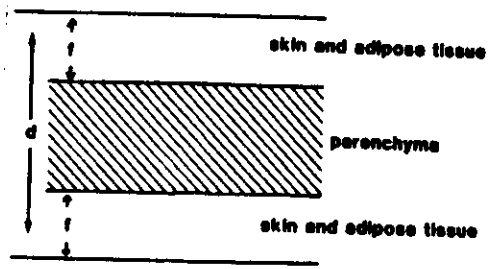

Fig. 9: Simple breast model

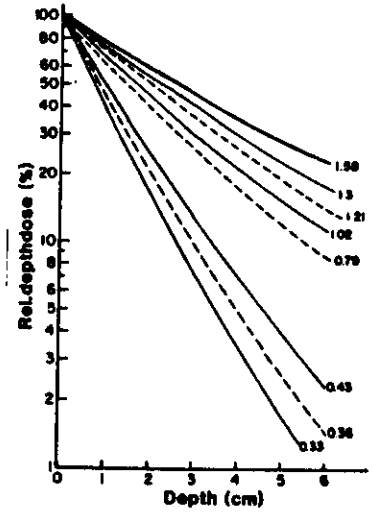

Fig. 10: Depth dose curves in breast tissue. The numbers represent the half value layer (mmAl)

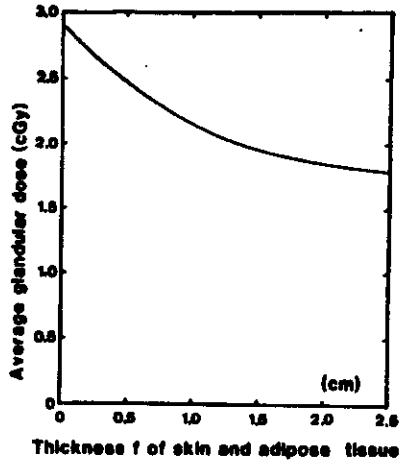

Fig. 11: Dependance of D_g from f /19/

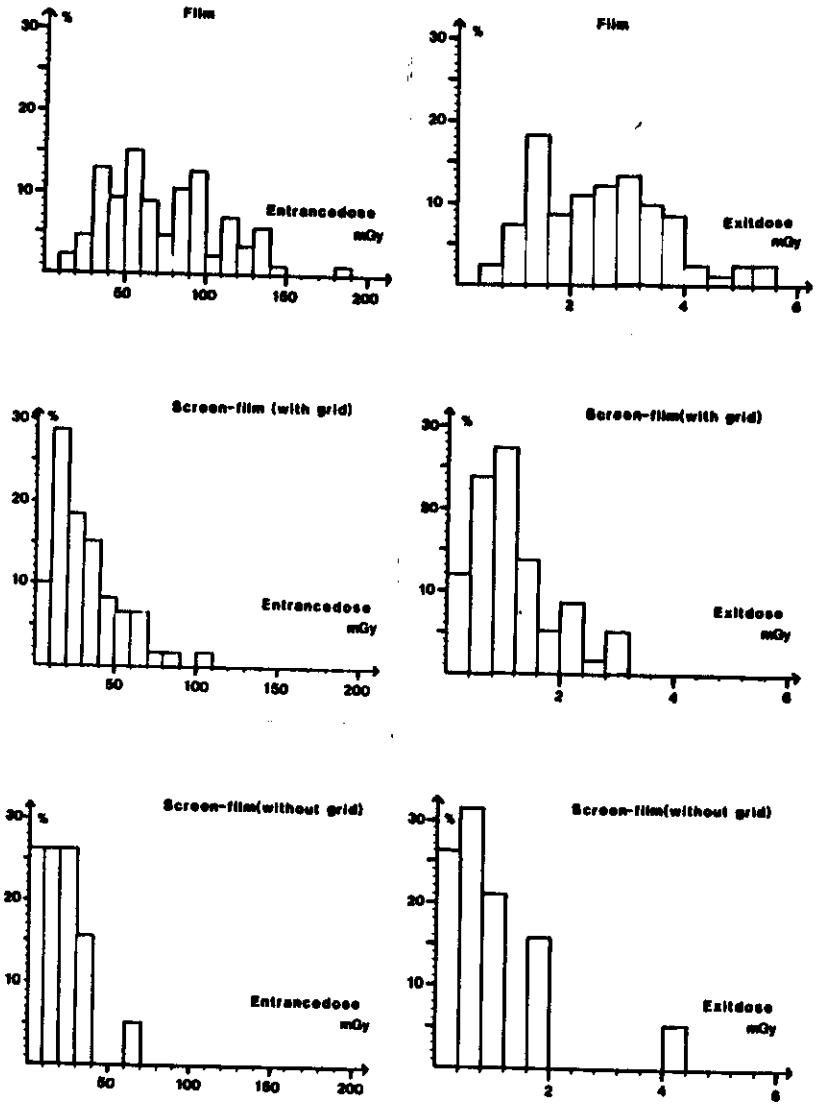

Fig. 12: Distributions of entrance- and exit doses